Detection of Neolithic Settlements in Thessaly, Greece through Multispectral and Hyperspectral Satellite Imagery

Dimitrios ALEXAKIS[1] – Apostolos SARRIS[2] – Theodoros ASTARAS[1,3] – Dimitrios OIKONOMIDIS[1]

[1]Remote Sensing and GIS Applications Laboratory, Department of Physical and Environmental Geography, School of Geology, Aristotle University of Thessaloniki, Thessaloniki 54124, Greece
[2]Laboratory of Geophysical – Satellite Remote Sensing & Archaeo-environment, Institute for Mediterranean Studies, Foundation for Research & Technology, Hellas (F.O.R.T.H.), Rethymno 74100, Crete, Greece
[1]alexakis@chania.teicrete.gr
[2]asaris@ret.forthnet.gr, www.ims.forth.gr
[3]astaras@geo.auth.gr

Abstract

Thessaly is a region of low relief in Greece where hundreds of Neolithic settlements/tells called *magoules* were established from the Early Neolithic period until the Bronze Age. Multi sensor remote sensing was applied to the study area in order to evaluate its potential to detect Neolithic settlements. Hundreds of sites were geo-referenced through systematic GPS surveying throughout the region. Data from 4 primary sensors were used, namely Landsat ETM, ASTER, EO1 - HYPERION and IKONOS. A range of image processing techniques were originally applied to the hyperspectral imagery in order to detect the settlements and validate the results of GPS surveying Although there are specific difficulties encountered in the classification of archaeological features composed by a similar parent material with the surrounding landscape, the results of the research suggested a different response of each sensor to the detection of the Neolithic settlements, according to its spectral and spatial resolution.

Keyword

Remote Sensing, Hyper-spectral imagery, Tells, Thessaly, Neolithic

1. Introduction

The spectral capability of early satellite sensors opened up new perspectives in the field of archaeological research. The recent availability of hyperspectral and multispectral satellite imageries has established a valid and low cost alternative to aerial imagery in the field of archaeological remote sensing. The high spatial resolution and spectral capability can make VHR satellite images a valuable data source for archaeological investigation ranging from synoptic view to small details (Masini and Lasaponara 2007).

In this study the satellite data will be statistically analysed together with other environmental parameters to examine any kind of correlation between environmental, archaeological and satellite data. The goal of the project is the application of different methods and means of satellite remote sensing for the detection of Neolithic settlements. Moreover we want to compare different methods and extract integrated methodologies for the detection of Neolithic settlements. Finally we wanted to assess the complementary use of different imagery for more satisfying results.

2. Research methods and materials

The study involved satellite image detection of Neolithic settlements in Thessaly by incorporating the following satellite and digital spatial data (*Table 1*):
– four ASTER images
– one LANDSAT ETM image
– one HYPERION image
– four IKONOS images
– five aerial photos
– The results of topographic mapping through systematic GPS surveying of more than 342 Neolithic settlements of Thessaly
– A DEM of 20m pixel size of the study area

3. Satellite image processing

The image processing of satellite data was carried out in two steps. First we started with the preprocessing

Sensor	Acquisition Date	Spatial Resolution (m)	Subsystem	Spectal Bands	Radiometric Resolution	Band range (nm)
Hyper - Spectal sensor						
1. Hyperion	September 3, 2001	30	VNIR, SWIR	137	16-bit	VNIR : 9-57 SWIR: 82-97, 101-119 135-164, 191-218
Hyper - Spatial sensors						
1. IKONOS	June 1, 2006	1	VNIR	4	11-bit	445 -516
	December 12, 2005					506-595
	March 1, 2007					632-698
	December 12, 2005		SWIR			757-853
	June 16, 2006					
Multi - Spectral Sensors						
1. Landsat - 7	July, 28, 1999	30	VNIR	7	8 -bit	450-515
						525-605
						630-690
			SWIR			750-900
						1550-1750
						2090-2350
		60	TIR			1040-1250
		15	Panchromatic			500-900
2. Aster	March, 19, 2003	15	VNIR	14	8-bit	520-600
	June, 30, 2004					630-690
	June, 30, 2003					780-860
	March, 19, 2003	30	SWIR			1600-1700
						2145-2185
						2185-2225
						2235-2285
						2295-2365
						2360-2430
		90	TIR		12-bit	8125-8475
						8475-8825
						8925-9275
						10250-10950
						10950-11650
Airphotos	January, 3, 1999,18 airphotos	1,5 m				

Table 1. Spectral, spatial and temporal attributes of the satellite sensors and aerial photos that were used for the study.

procedures and then we continued with the main image processing steps.

3.1. Preprocessing of satellite images

Before starting the image processing we masked the sea, the clouds and the snow areas of all the images. Then we proceeded to the construction of image mosaics (*Fig. 1*) and the transformation of the projection systems to a common projection system (EGSA87/HGSR87). The final step of image preprocessing was the conversion of DN values of images to reflectance. Initially we used different equations to convert the DN values to radiance. We converted the DN values

of ASTER images through the equation: *Lrad = (DN-1)*Unit Conversion Coefficient* (Smith 2001). For the IKONOS images we used the equation: *Lrad = DN/Unit Conversion Coefficient* (Fleming 2001*).* The conversion of DN values of Landsat images to radiance was accomplished through the equation: *Lrad = DN * Grescale + Brescale*, where *Grescale + Brescale* are band specific rescaling factors (Chander and Marcham 2003). In the case of HYPERION images "signal to noise" ratio was used to select 139 bands from the total of 220. Then we converted DN values to radiance values according to the equations: *VNIRL = DN /40, SWIRL = DN / 80* (USGS 2007). The last conversion had to do with the conversion of
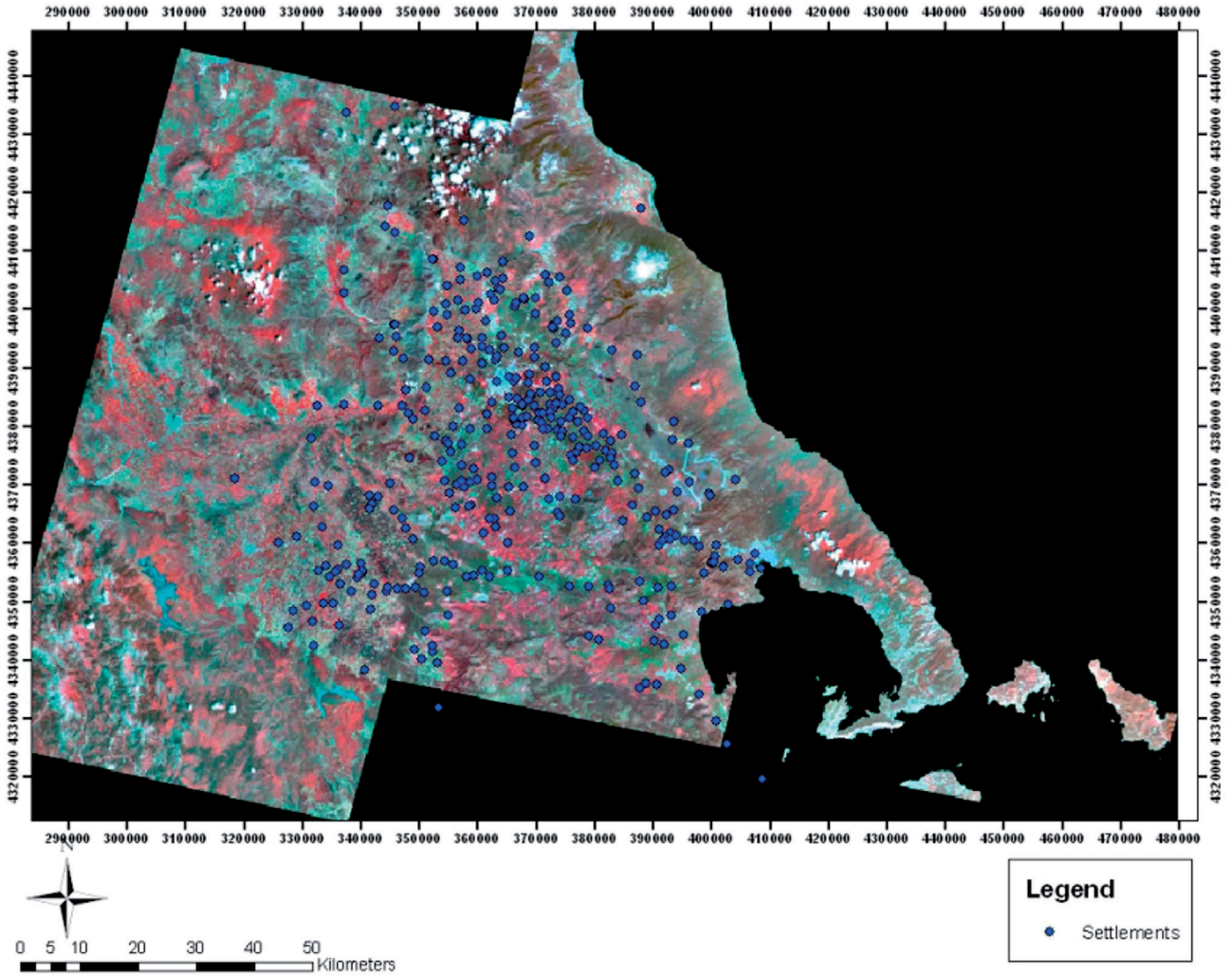
Fig. 1. Color composite RGB→3,2,1 of the mosaic of the four ASTER images used to cover the whole area of interest. The dots represent the location of the Neolithic magoules.

the radiance of all images to reflectance through the general algorithm:

$$Pp = \Pi\, L_\lambda\, d^2\, / ESUN\lambda\, \cos\theta_s$$

(Chander and Marcham 2003) where :

Pp is unitless planetary reflectance,
L_λ is spectral radiance at the sensor's aperture,
d^2 is the Earth–Sun distance in astronomical units,
$ESUN_\lambda$ is the mean solar exoatmospheric irradiance,
Θ_s is the solar zenith angle in degrees.

3.2. Composition of RGB Composites

Several RGB composites were constructed in an effort to examine their efficiency in the detection of Neolithic settlements. For the ASTER image with acquisition date 19-03-2003, where most of the magoules are registered, the RGB→1,2,3, RGB→3,2,5 and RGB→2,3,7 composites (*Fig. 2*) have been the most successful for the detection of

Neolithic settlements. (Out of 239 settlements 39 were highly visible, 49 average visible and 151 poorly visible. This categorization was accomplished after the interpretation regarding the appearance of each settlement after applying the spectral enhancement method of RGB composite.) Those composites appeared to have the highest Optimum Index Factor. High OIF values indicate bands that contain much "information" with little correlation. By using the OIF method, three band components of an RGB can be evaluated on their effectiveness for display (Buhe *et al.* 2006).

Similarly, RGB composites of IKONOS images were able to detect 27 in a total of 48 settlements. It has to be noted that 19 of the detectable magoulas, namely the highest of all corresponding to an average altitude of 4.6m, were highly visible in all RGB composites. On the other hand, RGB composites of Landsat and HYPERION images were not very promising (for HYPERION composites only five settlements were detected of a total of 21). Finally,
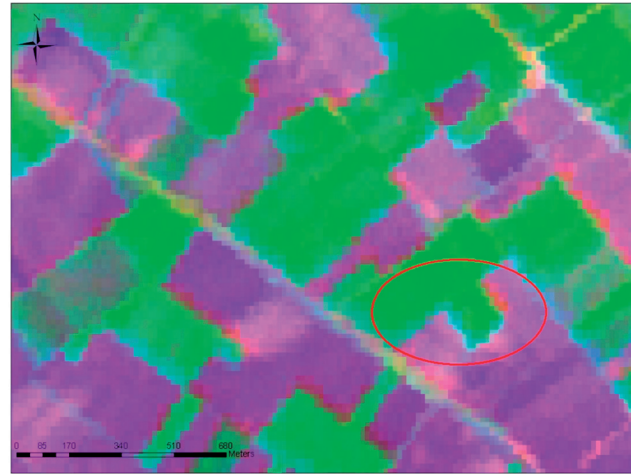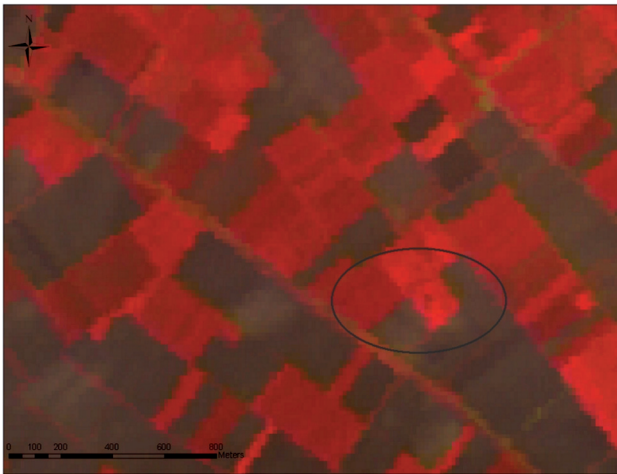
Fig. 2. RGB→3,2,5 of ASTER image − Settlement Melisa 1 (left). Right RGB→2,3,7 of ASTER image −
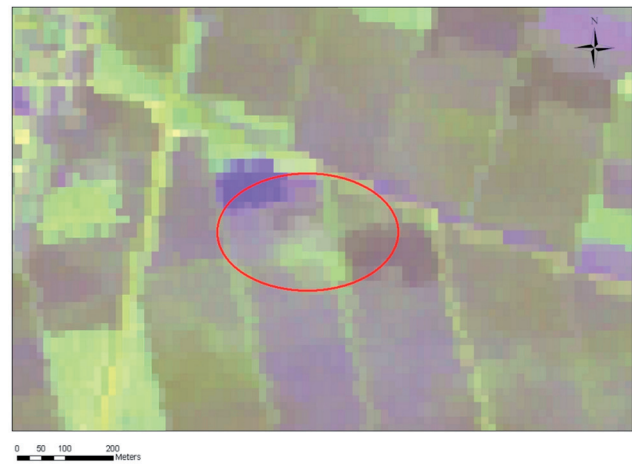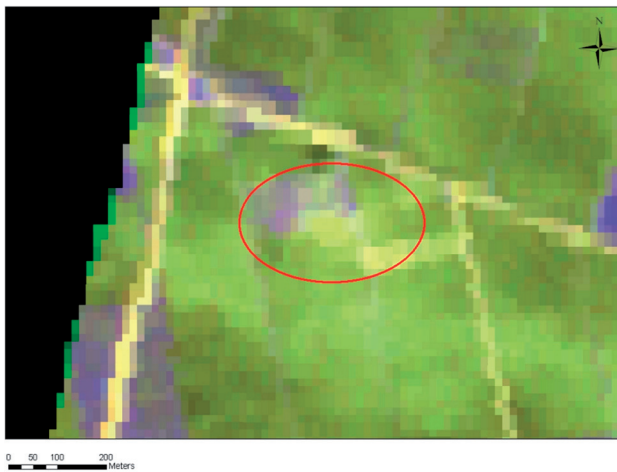*Settlement Melisa 1 (right).*

Fig. 3. Appearance of a settlement on the ASTER image with acquisition date 19-03-2003 (spring) (left).
Right: Appearance of the same settlement on 30−06-2004 (summer) (right).

average altitude aerial images contributed to an excellent detection of all the five settlements that were inside the spatial limits of the airphoto mosaic. As a general conclusion however, the most crucial factors for the detection of magoules proved to be the acquisition date of the image (best results during spring time) due to the fact that the majority of the settlements are cultivated (*Fig. 3*).

3.3. Spectral profile comparison and classification

The identification of spectral signatures was considered to be a crucial task for the detection of Neolithic settlements, especially for the classification process. That task was accomplished in order to exploit any potentially distinct spectral characteristics of surface and subsurface settlement patterns compared with the surrounding material (Rowlands and Sarris 2006). Signatures were collected from all the tells and

were divided in to two categories: those collected from plain areas and those collected from mountainous areas, due to different soil cover (*Fig. 4*).

The basic statistics for each band for all satellite images have been evaluated. Each band was reclassified into two categories: a) for all pixels within the range of <reflectance>+/-σ and b) for all the pixels outside the specific range. As a result, binary files were created and Boolean addition was followed to produce a classification map (*Fig. 5*).

3.4. Principal Component Analysis

Principal Component Analysis involves a mathematical procedure that transforms a number of correlated variables in a smaller number of uncorrelated variables called principal components. We applied PCA to ASTER, Landsat and Hyperion Images. PCA of ASTER images concluded to the best results where 39 settlements were highly
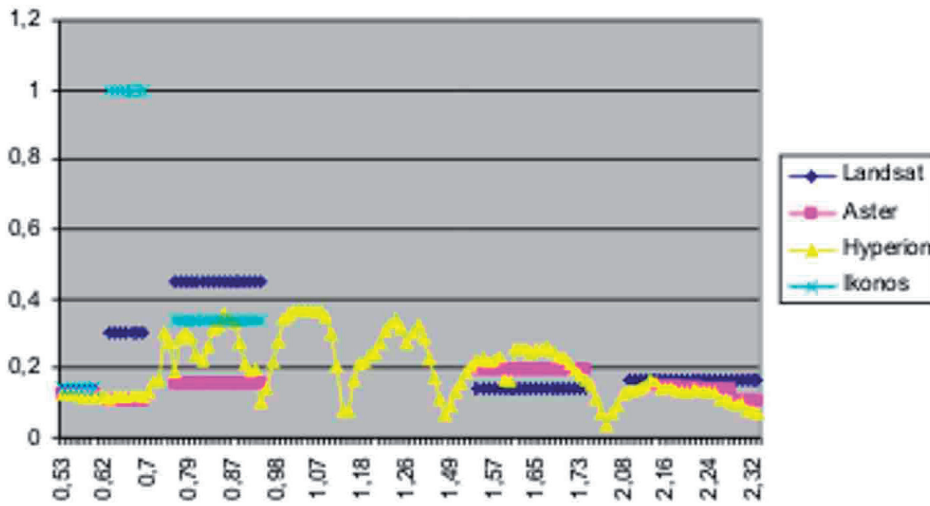
Fig. 4. Comparison of spectral signatures of all the sensors from the Neolithic settlements collected from the plains of Thessaly.

3.5. Data fusion

Image fusion is a standard satellite image procedure of combining images of different spatial resolution to obtain a single final composite image. The goal is to exploit the spectral and spatial characteristics of all images at the same time in order to accomplish the detection of as many settlements as possible. The images to be used can be from different sensors and of 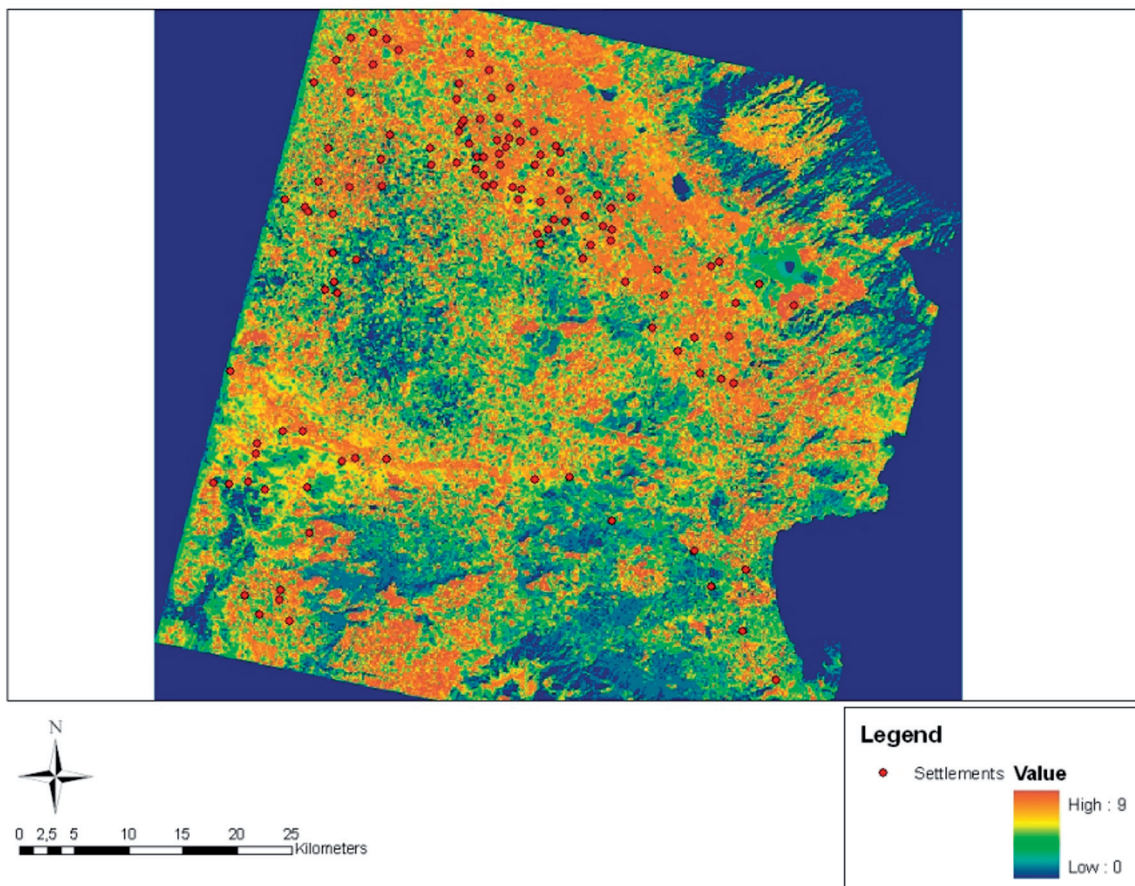different resolutions. Various fusion combinations were tried, such as ASTER (15m) visible channels with the PCA product of HYPERION (30m) or the high resolution (1m) bands of IKONOS with the PCA product of the HYPERION. The results were highly promising for the cases of fusion between high spatial resolution and high spectral resolution images (*Fig. 7*).

discriminated and 47 medium discriminated in a total of 247. Furthermore, 14 magoules that were not visible in the original images were clearly visible after applying PCA to ASTER images (*Fig. 6*).

Fig. 5. Classification map from the spectral signatures of ASTER images.
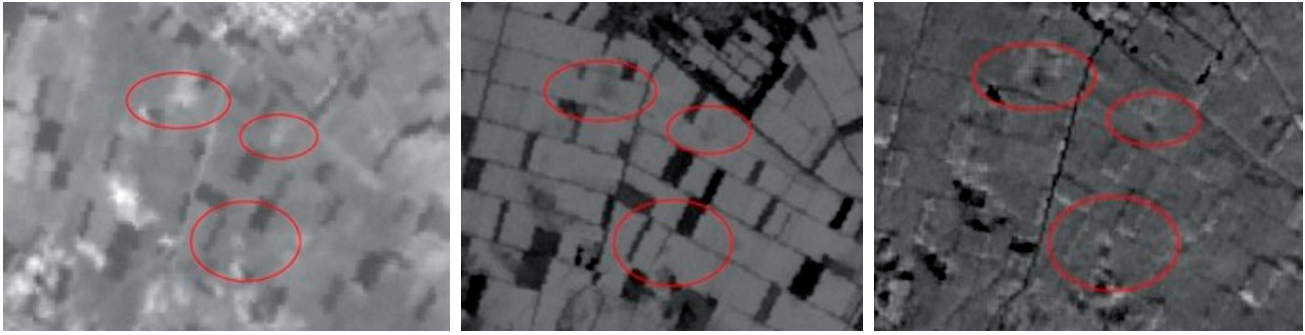
Fig. 6. Appearance of three settlements to the first Principal Component of ASTER image (left). Appearance of three settlements to the second Principal Component of ASTER image (middle). Appearance of three settlements to the third Principal Component of ASTER image (right).
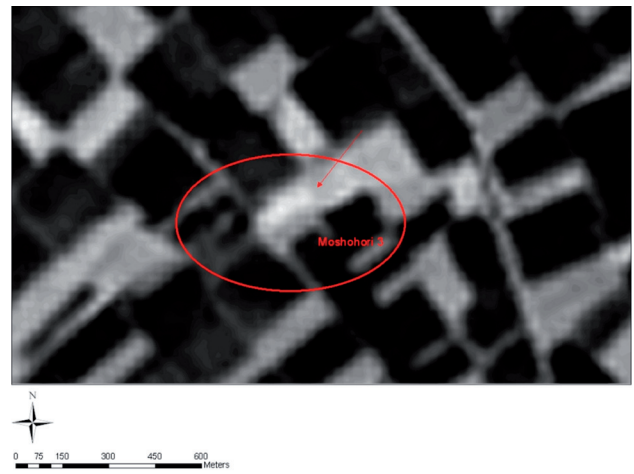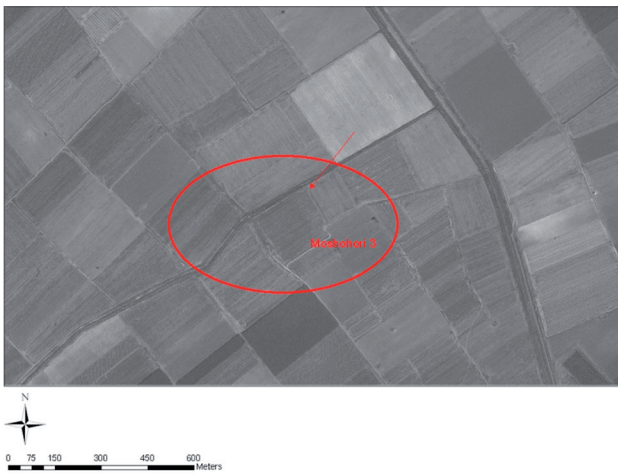

Fig. 7. Settlement Moshohori represented in an Ikonos image (left) and the same region after image fusion between IKONOS and HYPERION (right).

3.6. Spectral Mixer utility

In our effort to exploit the high spectral resolution of HYPERION images, we applied a spectral mixer application through the use of Erdas Imagine 9.1 software. Spectral Mixer produces three bands to be assigned to the red, green and blue colour guns, but in this case instead of just assigning each band

Fig. 8. Appearance of a settlement (RGB→8, 9, 10) before the application of Spectral Mixer utility (left). Appearance of the same settlement after the application of RGB 1 (right).

to a colour gun one can select a weighted average of spectral bands to be assigned to a colour gun (Erdas Field Guide 2006). For HYPERION images we used only the bands that have reflectance values above 0.3 and we assigned a weighting coefficient of 0.14 for each band. The new RGB that was created (RGB1) employed the mixing of the bands (38, 42,48, 49, 50, 51, 52), (85, 86, 87, 88, 89, 90, 91, 92,) and (93, 94, 108, 109, 110, 111, 113, 114) (*Fig. 8*).

3.7 Radiometric enhancement

Radiometric enhancement was vital for the appearance of the images. After applying radiometric enhancement to ASTER images (acquisition date 19-03-2003) we managed to detect 57 settlements. A non-linear radiometric enhancement of the HYPERION PCA image, followed by an inversion of brightness, was able to highlight eight settlements from a total of nine. (Melia 1, Melia 2, Anagennisi 2, Moshohori 3, Kipseli 2, Prodromos 1 of Larisa, Nikaia 17 and Kuparissia 2). A similar non-linear radiometric enhancement of the high resolution IKONOS images through the modification of the histogram was able to outline the round shape of known magoules, as well as to identify ten more targets of similar geometry that need to be verified by ground truthing activities that will follow (*Fig. 9*).
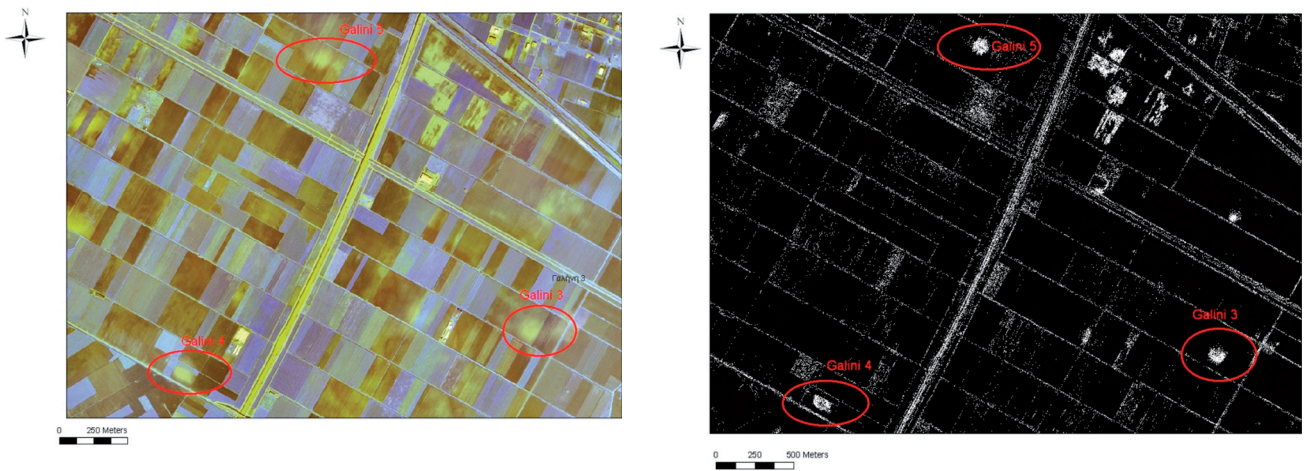

Fig. 9. Appearance of three settlements in the original IKONOS image (left) and the radiometrically enhanced image, where three Neolithic settlements are highlighted (right). To the north of Galini-3 settlement, shown at the lower right of the image, another smaller potential magoula is suggested.

Classification Method	Overall Accuracy (%)
Minimum Distance	78
Mahalanobis	80
Maximum Likelihood	84
Maximum Likelihood (fuzzy classification	90
Mahalanobis (fuzzy classification)	96
Minimum Distance (fuzzy classification	89
Spectral Angle Mapper	59
Parallilepiped	60

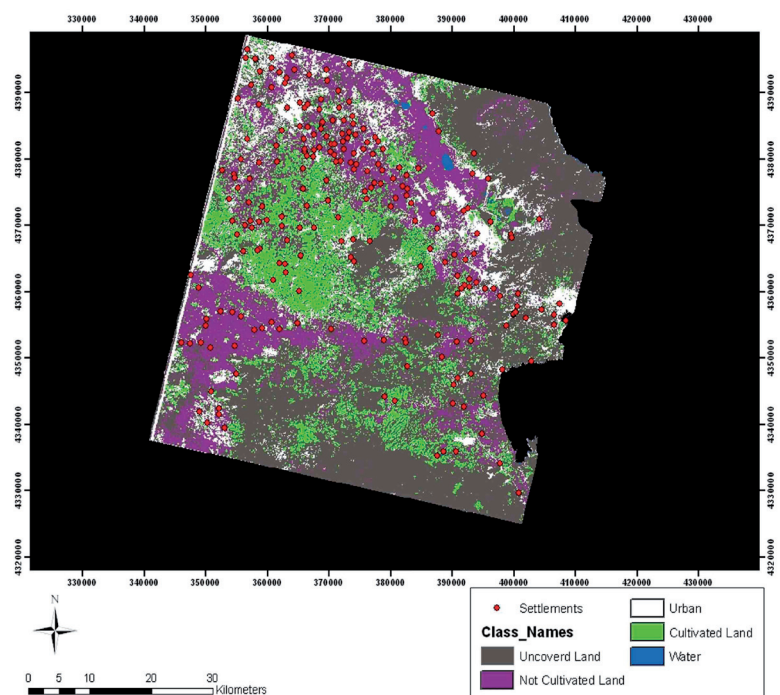*Table 2. Accuracy of each image classification method.*

Fig. 10. Results of the Land Classification of ASTER image through the use of Mahalanobis Distance (fuzzy) algorithm.
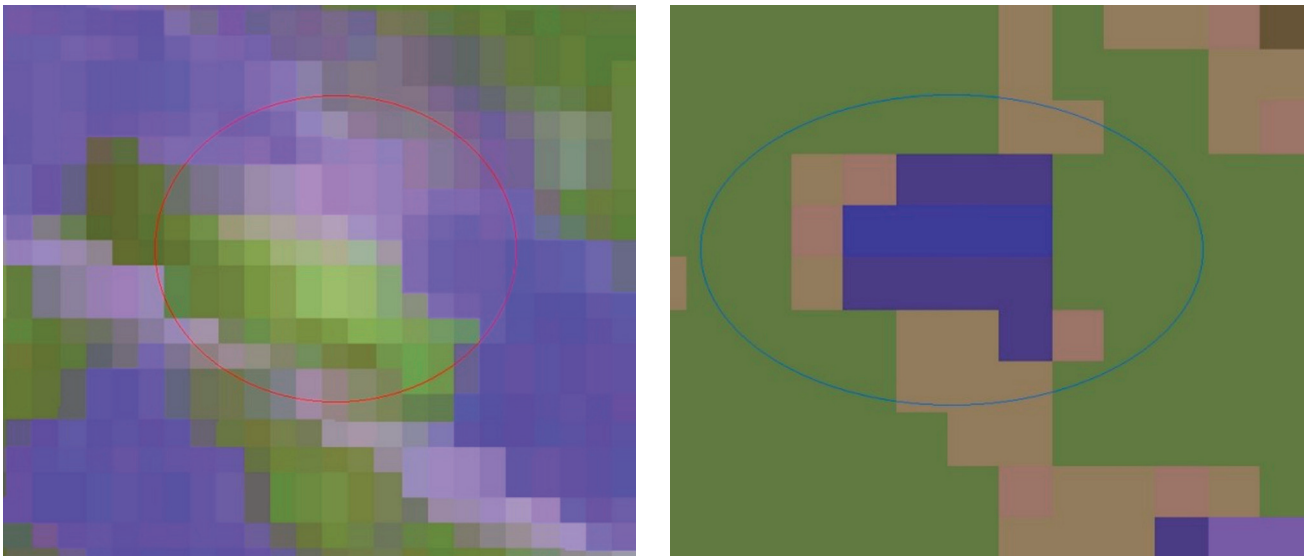
Fig. 11. Original ASTER (RGB→1,2,3) image indicating the settlement of Galini 4 (left) and the same area after the application of De-correlation Stretch (right).

3.8. Land classification and vegetation indices

In the domain of predictive modelling, the specification of the environmental attributes that correlate to the location of the archaeological sites is of great importance. For this reason, in order to investigate the land use regime of surrounding the magoules, several methods of supervised classification were applied to Landsat and ASTER images. Mahalanobis classification proved to be the most efficient one in terms of the overall accuracy assessment compared to all the classification algorithms that were applied (Maximum Likelihood, Minimum Distance, Mahalanobis Distance, Parallilepiped, Spectral Angle Mapper, Maximum Likelihood (fuzzy), Minimum Distance (fuzzy), Mahalanobis Distance (fuzzy)) (*Table 2* and *Fig. 10*).

Due to the small agreement between the land use classification results that produced between Landsat and ASTER sensors, the Normalised Difference Vegetation Index (NDVI) was computed to analyze the difference of vegetation during various acquisition dates. As expected, the NDVI of the spring ASTER image was higher than that of the summer Landsat image.

3.9. De-correlation stretch

The de-correlation stretch is a process that is used to enhance (stretch) the color differences found in the input pixels. The principal component transformation is similar, except that the transformation vectors are

derived from the correlation matrix rather than the covariance matrix. After we applied de-correlation stretch to the ASTER images, we managed not only to detect easily 36 Neolithic settlements (*Fig. 11*), but also to estimate the area of each settlement in a GIS environment.

3.10. Spatial enhancement

Spatial enhancement of images is considered to be a standard satellite image enhancement. Of the several types of filters that were applied in the specific study, only two of them, Sobel Right Diagonal 3×3 and Laplace 3×3 proved to be very useful for the detection of Neolithic settlements (*Fig. 12* and *Table 3*). The low number of detected settlements does not imply bad results for the method, taking into account the small spatial size of the settlements and the fact that the vast majority of them are continuously cultivated.

4. Predictive modeling

After applying all the above enhancement processes, a predictive model has been formed to locate potential magoules in the wider region of the Plain of Thessaly. The results of land use classification, NDVI estimates and those from the spectral signatures and classification of the ASTER image (acquisition date 19-03-2003) were combined with a DEM constructed by digitization of 1:50,000 scale topographic maps. All these data were reclassified and a certain weight factor was applied to each cell of the raster layers. The weight factor was selected after detailed
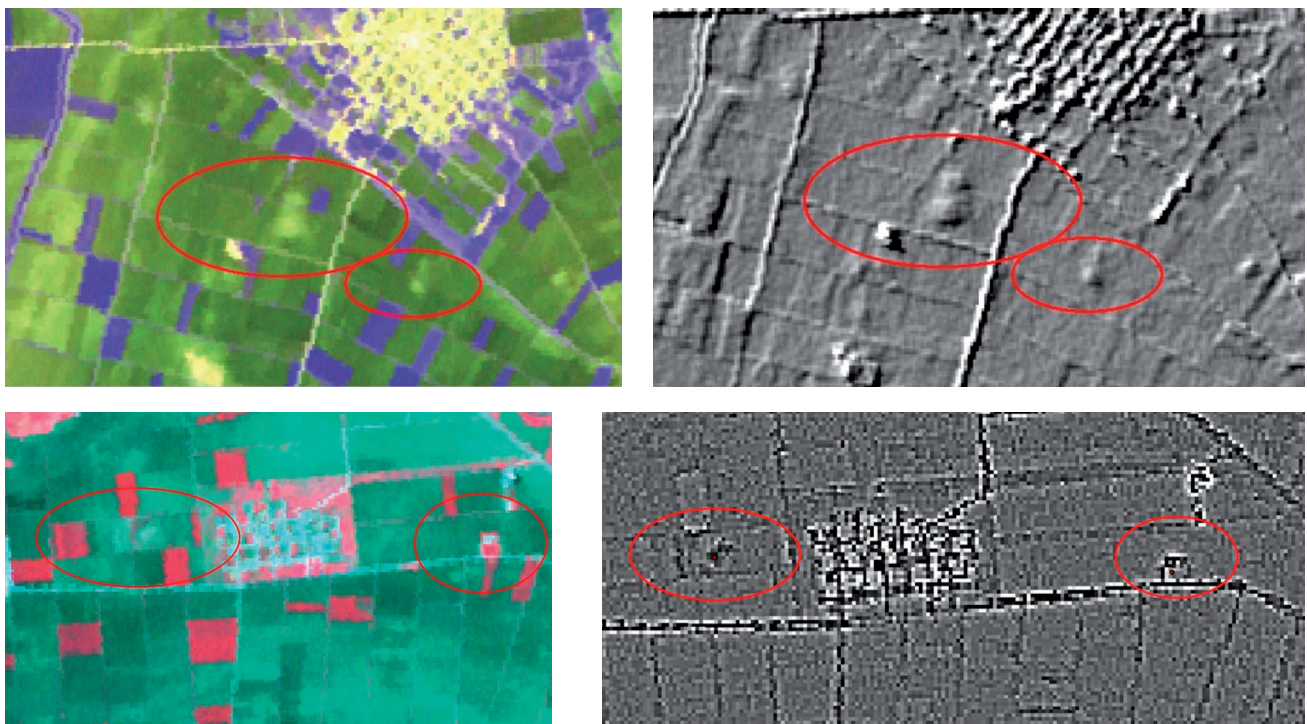
Fig. 12. Original ASTER image (RGB→1,2,3) around the Halki area (top left) and the corresponding image after the application of Sobel Right Diagonal filter (top right). Original ASTER image (RGB→1,2,3) around the settlements of Elliniko 1 and Elliniko 2 (bottom left) and the corresponding image after the application of Laplace Filter (bottom right).

ASTER IMAGE	Sobel Filter		Laplace Filter	
	Number of Settlements	Height (mean - meters)	Number of Settlements	Height (mean - meters)
Excellent Discrimination	59	4,37	40	5,15
Medium Discrimination	86	3,92	48	4,12
Bad Discrimination	69	3,51	121	3,14
Sum	211		211	
HYPERION IMAGE	Sobel Filter		Laplace Filter	
	Number of Settlements	Height (mean - meters)	Number of Settlements	Height (mean - meters)
Excellent Discrimination	6	3,8	40	5,15
Medium Discrimination	6	4,33	48	4,12
Bad Discrimination	7	3,57	121	3,14
Sum	19		211	
HYPERION IMAGE (FUSION)	Sobel Filter		Laplace Filter	
	Number of Settlements	Height (mean - meters)	Number of Settlements	Height (mean - meters)
Excellent Discrimination	9	5,88	40	5,15
Medium Discrimination	4	3	48	4,12
Bad Discrimination	5	1,8	121	3,14
Sum	18		211	

Table 3. The number of settlements that are enhanced after the application of different filters to various images.

examination of the statistics relating each factor with the establishment of settlement. All the raster layers were rated and the following equation was used through the raster calculator of ArcGIS 9.1 software to construct the final predictive model map (*Fig. 13*): Predictive Areas = DEM * 0.3 + Land Use * 0.5 + NDVI * 0.3 + Spectral Signature Map * 0.7

FACTORS	WEIGHTING	RATING
DEM		
Height< 120 m	9	0,3
120 - 200 m	6	
> 200	4	
NDVI		
> 0,2	8	0,5
0,2 - 0,3	6	
< 0,3	4	
LAND USE		0,5
Uncovered Land	7	
Urban	6	
Cultivated Land	5	
Not Cultivated Land	4	
SPECTRAL SIGNATURES	from 1 - 9	0,7

Table 4. Weights and rating for each factor.

After constructing the final map we estimated that 92 of the already known settlements are laid on areas of high probability and 23 in areas of medium probability.

Fig. 13. Map of predictive modelling.

5. Conclusions

An integration of images from different satellite sensors can contribute to a faster and more accurate and qualitative detection of archaeological sites. Specifically, ASTER images proved to be the most reliable and efficient for the detection of Neolithic settlements. In contrast, Landsat images concluded to quite poor results. The high spectral abilities of HYPERION, especially after merging it with the high resolution images of Ikonos, seem to have an increased potential not only in detecting but also in outlining the particular features. The image processes that proved to be more effective were spatial filtering, the process of de-correlation stretch and radiometric enhancement. The integration of land use classification data with NDVI and spectral signatures resulted in very promising modelling maps. Although the above processes were limited to the satellite imagery, it is expected that when combined with the results of the rest of the GIS spatial analyses, they will produce a more integrated methodology for the detection of magoules and the study of the Neolithic settlement patterns.

References

Buhe, Aosier, Tsuchiya Kimiyuki, Kaneko Masami, Ohtaishi Noriyuki and Mahmut Halik (2007). Cover of Oases and forest in XinJiang, China retrieved from ASTER data. *Advances in Space Research* 39, 39–45.
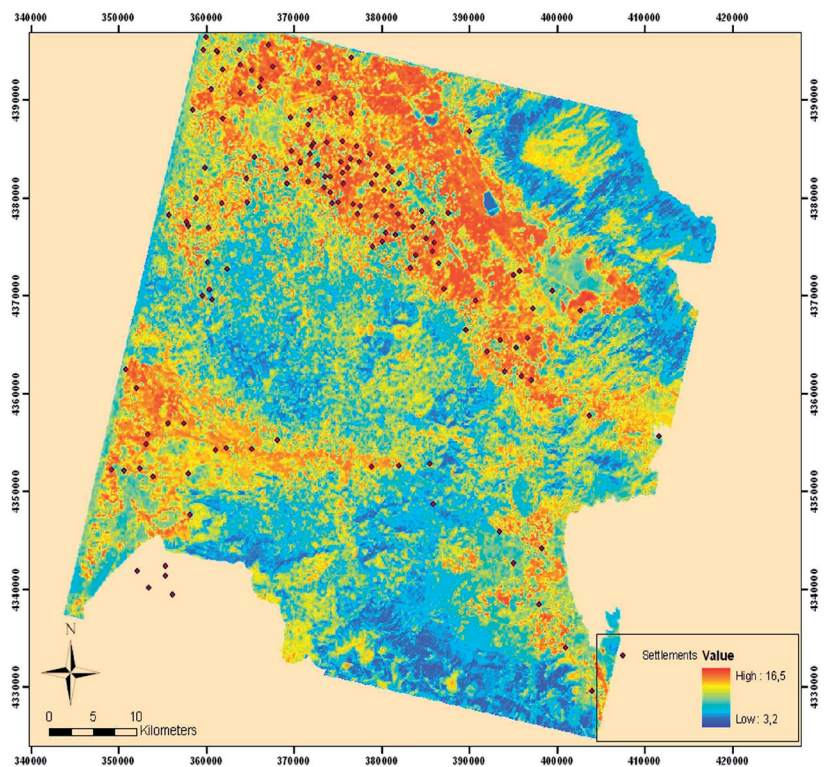
Chander, Gyanesh and Brian Markham (2003). Revised Landsat – 5 TM Radiometric Calibration Procedures and Postcalibration Dynamic Ranges. IEEE *Transactions on Geoscience and Remote Sensing* Vol 41, No 11, 1–4.

Erdas Field Guide (2006). Erdas Inc, Atlanta, Georgia.

Masini, Nicola and Rosa Lasaponara (2007). Investigating the spectral capability of Quickbird data to detect archaeological remains buried under vegetated and not vegetated areas. *Journal of Cultural Heritage* 8, 53–60.

Rowlands, Aled and Apostolos Sarris (2006). Detection of exposed and subsurface archaeological remains using multi – sensor remote sensing. *Journal of Archaeological Science* 34, 795–803.

Fleming, Danid (2001). Ikonos DN Value Conversion to Planetary Reflectance Values, CRESS Project, UMCP Geography, 1–4.

Smith, Akistair (2007). How to convert ASTER Radiance value to reflectance, University of Idaho, http://www.cnrhome.uidaho.edu/default.aspx?pid=85984

USGS -Earth Observing 1 (EO – 1) (2007). How are the radiance values (L) determined within the Hyperion bands? http://eo1.usgs.gov/faq.php?id=23